Title

The 6d {yields} 5f Fluorescence Spectra of PaCl{sub 6}{super 2-} in a Cs{sub 2}ZrCl{sub 6} Crystal

Journal

Journal of chemical physics, 94(2)

Authors

Piehler, D.
Kot, W.K.
Edelstein, N.

Publication Date

1990-08-01

LBL-29451
Preprint

Lawrence Berkeley Laboratory

UNIVERSITY OF CALIFORNIA

Materials & Chemical Sciences Division

Submitted to Journal of Chemical Physics

The 6d → 5f Fluorescence Spectra of $PaCl_6^{2-}$ in a Cs_2ZrCl_6 Crystal

D. Piehler, W.K. Kot, and N. Edelstein

August 1990

Prepared for the U.S. Department of Energy under Contract Number DE-AC03-76SF00098

DISCLAIMER

LBL-29451

The 6d → 5f Fluorescence Spectra of $PaCl_6^{2-}$ in a Cs_2ZrCl_6 Crystal

David Piehler, Wing K. Kot, and Norman Edelstein

Materials and Chemical Sciences Division

Lawrence Berkeley Laboratory

University of California

Berkeley, California 94720

This work was supported by the Director, Office of Energy Research, Office of Basic Energy Sciences, Chemical Sciences Division of the U.S. Department of Energy under Contract No. DE-AC03-76SF00098.

LBL-29451

The 6d → 5f Fluorescence Spectra of $PaCl_6^{2-}$ in a Cs_2ZrCl_6 Crystal

David Piehler, Wing K. Kot, and Norman Edelstein
Materials and Chemical Sciences Division
Lawrence Berkeley Laboratory
Berkeley, California 94720

Absract

Emission spectra from the parity-allowed electronic transitions between the lowest crystal field level of the $6d^1$ configuration to all the electronic levels of the $5f^1$ configuration of Pa^{4+} diluted into single crystals of Cs_2ZrCl_6 at 4.2 K show highly structured vibronic sidebands. Vibronic progressions are seen along the 310 cm^{-1} totally symmetric stretch of the $PaCl_6^{2-}$ complex. Most vibronic peaks correspond to even parity vibrations of the $PaCl_6^{2-}$ complex or the host lattice. Additionally, electronic Raman scattering was observed between the two lowest crystal field levels of the $5f^1$ configuration by exciting with an argon ion laser in near resonance with the lowest level of the $5d^1$ configuration.

Introduction

At the beginning of both the 4f and 5f electron series the various possible electronic configurations for atoms or ions with one electron outside the xenon and radon core are very close in energy.[1,2] Thus parity-allowed, interconfigurational optical transitions may be observed. For the Ce^{3+} ion, the ground state has a $4f^1$ configuration and the excited $5d^1$ configuration begins at ~ 20000-40000 cm^{-1}, depending on the environment surrounding the Ce^{3+} ion.[3] An analogous situation exists for the $5f^1$ and $6d^1$ configurations of the Pa^{4+} ion which makes it an attractive ion to study spectroscopically. Ryan has tabulated the difference in energies between the ground $5f^1$ state and the beginning of the excited $6d^1$ levels for the sparse solution data available.[4]

The first solid state studies of the optical and magnetic properties of the Pa^{4+} ion were reported by Axe, et al. The Pa^{4+} ion was incorporated as an impurity in Cs_2ZrCl_6 replacing a Zr^{4+} ion at a site of O_h symmetry. The electron paramagnetic resonance (EPR) spectrum at 4.2 K and the near-infrared absorption spectra were measured and the data analyzed in terms of the crystal field and spin-orbit interactions for a $5f^1$ electron.[5,6]

Additional optical studies have been reported for pure Pa^{4+} hexahalo compounds[7,8] and for the Pa^{4+} ion diluted in single crystals of $ThBr_4$ and $ThCl_4$.[9] In the latter work EPR results were also given. Naik and Krupa[10] reported absorption and fluorescence for $Pa^{4+}/ThBr_4$ and assigned the strong visible absorption bands at ~20,000 cm^{-1} to the $5f \rightarrow 6d$ interconfigurational transitions. Subsequently, Edelstein et al. analyzed the $5f \rightarrow 6d$ absorption spectra of Pa^{4+} in solutions of hexachloro and hexbromo salts and in single crystals of $ThBr_4$.[11]

One notable feature of the $Pa^{4+}/ThBr_4$ and $Pa^{4+}/ThCl_4$ studies was the strong fluorescence observed upon excitation with radiation above the onset of the 6d bands. Since the energy gap between the 6d and 5f configurations for Pa^{4+} in both $ThCl_4$ ($ThBr_4$) and $PaCl_6^{2-}$ are similar, strong fluorescence is to be expected upon excitation of the 6d bands in Pa^{4+}/Cs_2ZrCl_6. We report the results of such experiments in this paper.

Experimental

$ZrCl_4$ purchased from Alfa Inorganics (purity > 99.9%) was received in a bottle packed under argon. The bottle was transferred into an inert atmosphere box where about 20 grams was placed in a sublimation tube. This tube was transferred to a vacuum line (~ 10^{-2} mmHg) and the $ZrCl_4$ was sublimed at approximately 500°C. CsCl was placed in a tube on a vacuum line and heated under vacuum to 200°C. Stoichiometric amounts of dried CsCl and sublimed $ZrCl_4$ were weighed, thoroughly ground and mixed in an inert atmosphere box, then transferred into a quartz tube and sealed under vacuum. The sealed tube was then passed through a furnace at a rate of 2 mm/hour. The temperature of the

center region of the furnace was stabilized at 870°C. Clear single crystals of Cs_2ZrCl_6 were obtained by this method and their identity verified by powder x-ray diffraction patterns. Approximately 2 grams of this material was transferred to another quartz tube and 10 mg of ^{231}Pa was added in a "hot" inert atmosphere box. This tube was sealed under vacuum and passed through the furnace as described above. The ^{231}Pa used in the experiment was prepared by dissolving Pa_2O_5 in 10 M HF and precipitating with concentrated ammonia. The ppt. was rinsed with distilled water, acetone, and then dried in air at a temperature of 250°C. A bright yellow crystal was obtained by this method which showed an EPR spectrum of Pa^{4+}/Cs_2ZrCl_6 as reported by Axe, et al.[6] The exact mechanism and extent of the reduction of Pa^{5+} to the tetravalent state are not known. An impurity of Pa^{5+} will not affect the experiments described in this paper.

Part of the yellow Pa^{4+}/Cs_2ZrCl_6 was placed in a quartz tube, evacuated, and then refilled with about 200 Torr of He gas after which the quartz tube was sealed. The tube plus sample was placed in an Oxford CF 1204 optical cryostat and cooled to 4.2 K. An argon ion laser was used as an excitation source. Emission or electronic Raman spectra were analyzed by a SPEX Industries 1403 double monochromator and detected with a cooled Hamamatsu 943 photomultiplier tube. The bandwidth of the monochromator was about 1.5 cm^{-1} and the absolute accuracy was about 2 cm^{-1}. Below 11,100 cm^{-1} the sensitivity of the photomultiplier tube decreased rapidly, which resulted in a loss of intensity in this spectral region.

Review of Theory

The Hamiltonian for the energy levels of an f electron in octahedral symmetry may be written as

$$\mathcal{H} = \mathcal{H}_{SO} + \mathcal{H}_{CF}$$

$$\mathcal{H}_{SO} = \zeta_{\ell}(r)\vec{\ell}\cdot\vec{s}$$

$$\mathcal{H}_{CF} = B_0^4[C_0^4 + \frac{\sqrt{5}}{14}(C_{-4}^4 + C_4^4)] + B_0^6[C_0^6 - \frac{\sqrt{7}}{2}(C_{-4}^6 + C_4^6)]. \qquad (1)$$

The effects due to the radial part of the 5f wavefunctions are contained in the crystal field parameters B_0^4 and B_0^6, and the spin-orbit coupling constant $\zeta_{5f}(r)$, which are evaluated empirically. The matrix elements for the angular momentum operators, $\vec{s}$ and $\vec{\ell}$, and the tensor operators, C_q^k, depend only on the angular coordinates and are evaluated by standard techniques.[12]

Under the effect of the octahedral crystal field at the Pa^{4+} site, the seven degenerate f orbitals (of the free ion) decompose into two triplet states, Γ_4 and Γ_5, and one singlet state, Γ_2 (O_h point group). The energies of these levels can be written in terms of the energy splittings θ and Δ, when the spin-orbit coupling constant is assumed to be zero, or equivalently in terms of B_0^4 and B_0^6 as given in the Hamiltonian. When the electron spin is considered, each orbital becomes doubly degenerate and the double group representations Γ_{6u}, Γ_{7u}, and Γ_{8u} become the proper labels for the eigenstates and energy levels. Because the spin-orbit coupling interaction is large compared to the crystal field interaction, the crystal field levels fall in two groups which can be described (approximately) by the term labels $^2F_{5/2}$ and $^2F_{7/2}$. Table 1 gives the energy matrices of the levels and the ground state g value in terms of the parameters ζ_{5f}, Δ, and θ, and the conversion to B_0^4, and B_0^6.[7,13]

Unlike the 5f configuration, the radial wavefunction of the 6d configuration extends significantly beyond the filled $6s^26p^6$ shells of the Rn core. For this reason the 6d electron experiences a crystal field that is much larger than the 6d spin-orbit coupling. The octahedral (O_h) crystal field of $PaCl_6^{2-}$ splits the 6d configuration into two levels, a T_{2g} lower state (triply degenerate) and an E_g upper state (doubly degenerate). When the 6d spin-orbit interaction is included, the T_{2g} level splits into a Γ_{8g} (a degenerate quartet with the inclusion of spin) state and a higher-lying Γ_{7g} (Kramers doublet) state. The higher-lying E_g level also transforms as a Γ_{8g} quartet when the electron spin is considered. The splitting of the T_{2g} state (the energy difference between the Γ_{8g} and Γ_{7g} levels) was measured as approximately 3560 cm^{-1} from the solution spectrum of $PaCl_6^{2-}$ from which the value of ζ_{6d} = 2021 cm^{-1} was obtained. A lower limit of ~ 13800 cm^{-1} was obtained

for the 6d crystal field splitting of $PaCl_6^{2-}$.[11] The Hamiltonian of Eq. 1 also may be used for the 6d configuration. For a d^N configuration, $B_0^6 = 0$, so the energies are determined by the parameters $B_0^4(d)$ and ζ_{6d}.

A schematic energy level diagram showing the 5f and 6d levels for the $PaCl_6^{2-}$ ion, taken from Axe's data and the room temperature optical spectrum of Cs_2PaCl_6 in acetonitrile solution, is shown in Fig. 1.[5,11]

The wavefunctions obtained from Eq. 1 represent only the pure electronic wavefunctions and do not consider vibronic coupling. The intensity of an electronic transition from initial state i to the final state f may be written in the adiabatic approximation (which assumes the electronic part of the wavefunction is independent of the vibrational coordinates) as

$$I \propto |\langle i|e\vec{r}|f\rangle\langle \ell|m\rangle|^2 \qquad (2)$$

where I is the intensity, $e\vec{r}$ the electric dipole operator, and ℓ and m are the initial and final vibrational states, respectively. If it is further assumed that electronic-vibrational coupling is small and linear (i.e., the vibrational frequencies in the ground and excited states are equal), then for the case where only the lowest electronic energy level is populated, then

$$I_n \propto e^{-S}\left(\frac{S^n}{n!}\right) \qquad (3)$$

where S is the Huang-Rhys parameter and n is the vibrational quantum number of the terminal state. The deformation energy of the vibrational mode is then given by

$$\Delta E(\Gamma_i) = S\hbar\omega_i \qquad (4)$$

From equation 3 the Huang-Rhys parameter can be evaluated from a harmonic progression in a vibrational mode, and from its value the deformation energy may be estimated (Eq. 4). For the vibration corresponding to the normal coordinate Q_i,

$$S = 1/2\, Q_i^2 \omega_i^2 / \hbar. \qquad (5)$$

where M is the effective mass. Q_i, which corresponds to the totally symmetric vibrational mode, is the difference between the equilibrium distances of the metal ion and the ligand in the ground and excited states.[14,15]

Resonant Electronic Raman Scattering

The cross section σ for electronic Raman scattering[16] may be written as:

$$\sigma \propto \omega_s^3 \omega_l \left| \sum_n \frac{\langle i|e\vec{r}|n\rangle\langle n|e\vec{r}|f\rangle}{\omega_l - \omega_n} \right|^2 \qquad (6)$$

where ω_s and ω_l are the angular frequencies of the scattered and incident laser radiation, i and f are the initial and final states of the ground configuration, and $e\vec{r}$ is the electric dipole operator as before. Only the intermediate states $|n\rangle$, which represent states from configurations which have the opposite parity to the ground configuration, contribute to the above sum.

For most ions with an f^N ground configuration (N = 1-13), $\omega_n \sim 50{,}000$ cm^{-1}, $\omega_l \sim 20{,}000$ cm^{-1}, and the denominator in Eq. 6 is $\omega_l - \omega_n = \Delta\omega_{NR} \sim 30{,}000$ cm^{-1}. However for Pa^{4+}, $\omega_{6d} \approx 20{,}000$, $\omega_l \approx 19{,}500$ cm^{-1} and $\omega_l - \omega_n = \Delta\omega_R \sim 1000$ cm^{-1}. Therefore for Pa^{4+} the resonant enhancement of the electronic Raman scattering should be

$$\frac{I_R}{I_{NR}} \propto \left(\frac{\Delta\omega_{NR}}{\Delta\omega_R}\right)^2 \approx 1000.$$

Selection Rules

The emission spectra reported in this paper originate in the lowest 6d level of Γ_{8g} symmetry and terminate in all the crystal field levels of the 5f configuration which are of Γ_{6u}, Γ_{7u}, or Γ_{8u}, symmetry. The electric dipole operator transforms as Γ_{4u}. The direct product

$$\Gamma_{8g} \times \Gamma_{4u} \times (\Gamma_{6u}, \Gamma_{7u} \text{ or } \Gamma_{8u})$$

contains the irreducible representations Γ_{1g}, Γ_{2g}, Γ_{3g}, Γ_{4g}, and Γ_{5g} so the purely electronic (zero phonon) transition as well as the electronic transitions coupled to even parity phonons are allowed to each of the 5f levels.

The six local modes of the $PaCl_6^{2-}$ complex are labelled $\nu_1(\Gamma_{1g}$ or $a_{1g})$, $\nu_2(\Gamma_{3g}$ or $e_g)$, $\nu_3(\Gamma_{4u}$ or $t_{1u})$, $\nu_4(\Gamma_{4u}$ or $t_{1u})$, $\nu_5(\Gamma_{5g}$ or $t_{2g})$, and $\nu_6(\Gamma_{5u}$ or $t_{2u})$ where the symbols in the parentheses give the symmetries of normal modes in two equivalent O_h group notations. Unit cell group analysis indicates there are three additional vibrational modes arising from the motion of the host lattice: $\nu_{L1}(\Gamma_{4g}$ or $t_{1g})$, $\nu_{L2}(\Gamma_{5g}$ or $t_{2g})$, and $\nu_{L3}(\Gamma_{4u}$ or $t_{1u})$. Thus it is expected that the five even parity vibrations ν_{L1}, ν_{L2}, ν_1, ν_2, and ν_5 should contribute to the vibronic sidebands.[17]

Previous infrared and Raman results for the $AnCl_6^{2-}$ complexes ($An^{4+} = Th^{4+}$, Pa^{4+}, U^{4+}, Np^{4+}) indicate that $\nu_1 \approx 300$ cm^{-1}, $\nu_2 \approx 260$ cm^{-1}, and $\nu_5 \approx 120$ cm^{-1}.[18] For Cs_2ZrCl_6, $\nu_{L2} \approx 48$ cm^{-1}.[19] ν_{L1} is unknown since it is neither Raman or infra-red active. Combination bands may also be present in the vibronic sideband.

Results and Discussion

When the Pa^{4+}/Cs_2ZrCl_6 crystal at 4.2 K was irradiated with the 488 nm (20486.7 cm^{-1}) line of the argon ion laser, emission spectra were recorded from the lowest 6d level of Pa^{4+} to all the 5f levels as shown in Fig. 2-4. Shifting the argon ion laser to higher energies did not change the observed fluorescence. Five groups of bands were observed which are assigned as transitions from the lowest $6d(\Gamma_{8g})$ level to the five 5f levels (see Fig. 1). The emission spectra show highly structured vibronic sidebands in the green and yellow regions corresponding to the $6d(\Gamma_{8g}) \rightarrow {}^2F_{5/2}(\Gamma_{7u})$ (Fig. 2) and $6d(\Gamma_{8g}) \rightarrow {}^2F_{5/2}(\Gamma_{8u})$ (Fig. 3) transitions respectively. In Fig. 2, the zero phonon line at 19954 cm^{-1} shows a loss of intensity due to self absorption. In the near infrared region, emission bands corresponding to $6d(\Gamma_{8g}) \rightarrow {}^2F_{7/2}(\Gamma_{8u}')$ and $6d(\Gamma_{8g}) \rightarrow {}^2F_{7/2}(\Gamma_{6u})$ are shown in Fig. 4. The vibronic transitions for these transitions somewhat overlap. The $6d(\Gamma_{8g}) \rightarrow$

$^2F_{7/2}(\Gamma'_{7u})$ emission spectrum shown in Fig. 5 is featureless and much lower in intensity than the other emission bands.

Resonantly enhanced electronic Raman scattering (ERS) between the crystal field levels of the (primarily) $^2F_{5/2}$ manifold was obtained by excitation with 514.5 nm (19429.7 cm^{-1}) argon ion line. The spectrum is shown in Fig. 6. No ERS was observed terminating in the higher-lying multiplet. The energy of the $^2F_{5/2}(\Gamma_{8u})$ level obtained from the ERS experiment agrees quite well with the value obtained from the fluorescence experiment.

For a 5f or 6d electronic configuration only states which have (Γ_{8u}) or (Γ_{8g}) symmetry are subject to a dynamic Jahn-Teller distortion. Because the observed zero phonon lines and phonon sidebands are similar for each of 5f levels (of Γ_{6u}, Γ_{7u}, or Γ_{8u} symmetry) where structure is observed, the electronic-vibronic coupling which causes the structure must originate in the excited 6d(Γ_{8g}) level. No evidence is observed for a Jahn-Teller distortion in ground 5f configuration.

The most prominent feature in the emission spectra is the vibronic progression with a frequency of 310 cm^{-1}. The main peaks in the progression may be measured quite accurately. The weaker peaks in the sidebands are generally broader, overlap with other peaks, and so are more difficult to measure accurately. The energies of the zero phonon lines and the sidebands are given in Table 2.

The phonon lines allowed by the selection rules are the $\nu_1(a_{1g})$, $\nu_2(e_g)$ and $\nu_5(t_{2g})$ normal modes of the $PaCl_6^{2-}$ complex and from Table 2 are assigned to 310 cm^{-1}, ν_1; 253 $\pm$ 3 cm^{-1}, ν_2; and 125 $\pm$ 3 cm^{-1}, ν_5. The lattice modes are assigned as 34 $\pm$ 4 cm^{-1}, ν_{L1}; and 48 $\pm$ 3 cm^{-1}, ν_{L2}. Two other prominent features in the vibronic sidebands occur at ν = ~ 100 cm^{-1} and ν = 170 cm^{-1} and are probably combination bands. The $\nu \approx 100$ cm^{-1} could be assigned as $2\nu_{L2}$ or $3\nu_{L1}$ while the ν_{170} band is most likely $\nu_5 + \nu_{L2}$.

By use of Eq. 3 and the integration of the area for each of the vibronic peaks of the 310 cm^{-1} mode, the value of $S(a_{1g}) = 1.84$ is obtained. Figure 7 shows the comparison of the experimental and calculated intensities for the 17847 cm^{-1} fluorescence band (Fig. 3).

From this value of $S(a_{1g})$ the increase of the Pa-Cl bond in the 6d state is calculated to be ~ 0.1 Å.

A limited vibrational progression may be observed for the t_{2g} and e_g modes consisting of the 0th and 1st vibrational quanta. These same vibrational progressions also are found based on the 310 cm^{-1} harmonics. Values of the Huang-Rhys parameter for the e_g and t_{2g} modes may be estimated based on the relative intensities of

$$S = \frac{I(n\times 310 + \nu_{(t_{2g} \text{ or } e_g)})}{I(n\times 310)}$$

where n in this case is the vibrational quantum number for the 310 cm^{-1} vibration. For n = 0, the intensity of the zero phonon line is used. From these S values [$S(e_g) = 0.11$, $S(t_{2g}) = 0.33$] the distortion energies due to the dynamic Jahn-Teller effect are:

$$\Gamma_{8g} - e_g,\ \hbar\omega_{e_g} = 250\ cm^{-1},\ E_{dis}(e_g) \cong 28\ cm^{-1}$$
$$\Gamma_{8g} - t_{2g},\ \hbar\omega_{t_{2g}} = 125\ cm^{-1},\ E_{dis}(t_{2g}) \cong 41\ cm^{-1}$$

The distortion energies calculated from this model for the e_g and t_{2g} modes are rather small. Warren[20] has pointed out that for a Γ_{8g} electronic state, these energies are reduced to 25% of their values for a T_{2g} electronic ground state.

Electronic Structure

The energies and assignments of four of the five 5f levels can be obtained from the data of Table 2. The energy of the Γ_{7u}' state is uncertain because of the low intensity of this emission line. Axe assigned the energy of this level at 5210 cm^{-1} with an estimated error of ± 200 cm^{-1}.[5] Edelstein et al. assigned this level at 5333 ± 5 cm^{-1} from the absorption spectrum of the pure compound $(Et_4N)_2PaCl_6$.[7] The present data (Fig. 5) indicate that the $\Gamma_{7u} \rightarrow \Gamma_{7u}'$ transition is at 5350 ± 50 cm^{-1} in Pa^{4+}/Cs_2ZrCl_6.

There are three parameters in the Hamiltonian of Eq. 4 which can be fit exactly by using the energies of the Γ_{8u}, Γ_{8u}', and Γ_{6u} states. The calculated and experimental values are shown in Table 3. Note the experimental energy of the Γ_{7u}' state (even with a large error) and the g value of the ground state are not reproduced. Clearly the Hamiltonian of Eq. 1 is not adequate for this simple system. However, the 5f wavefunctions given by the above fitting procedure plus the 6d wavefunctions obtained from the parameters given by Edelstein et al. in Table IV of Ref. 11 for Cs_2PaCl_6 have been used to calculate the relative intensities of the transitions from the 6d(Γ_{8g}) level to all the 5f levels. The calculated relative values are compared with experimental relative intensities in Table 4.

The most striking result shown in Table 4 is the very weak relative intensity for the transition to the Γ_{7u}' state. The transitions to the 5f J = 7/2 levels were expected to be weaker than to the 5f J = 5/2 states since there is a $\Delta J = \pm 1$ selection rule for electric dipole transitions and the 6d(Γ_{8g}) eigenstate has a 77% J = 3/2 component. The agreement between the calculated and experimental relative values is quite satisfactory.

Conclusion

Four levels of the 5f configuration of Pa^{4+}/Cs_2ZrCl_6 have been accurately measured as well as the lowest Γ_{8g} level of the excited 6d configuration by fluorescence. An analysis of vibronic structure indicates that the Pa-Cl bond distance is ~ 0.1 Å longer in the 6d excited states. Estimates have been given of Jahn-Teller distortion energies in 6d(Γ_{8g}) quartet for the e_g and t_{2g} vibrations. The simple crystal field model can not accurately produce the energies of the 5f configuration and the g value of the ground state. The relative strengths of the fluorescent bands are reproduced quite well by a calculation of the relative electric dipole intensities between the 6d(Γ_{8g}) state and the 5f levels.

Acknowledgement.

We wish to thank Professor D.S. McClure for helpful discussions. This work was supported by the Director, Office of Energy Research, Office of Basic Energy Sciences, Chemical Sciences Division of the U.S. Department of Energy under Contract No. DE-AC03-76SF00098.

References

1. W.C. Martin, R. Zalubas, and L. Hagan, "Atomic Energy Levels - The Rare-Earth Elements," NSRDS-NBS (60), 1978.
2. M. Fred in "The Chemistry of the Actinide Elements," J.J. Katz, G.T. Seaborg, and L.R. Morss, Ed., 2nd Ed., Chapman and Hall, London, 1986, pp. 1224-1226.
3. G.M. Williams, N. Edelstein, L.A. Boatner, and M.M. Abraham, Phys. Rev. B, 40, 4143 (1989).
4. R.L. Ryan in "Lanthanides and Actinides," K.W. Bagnall, Ed. MTP International Review of Science, Series 1, Buttersworth, London, 1972, p. 358.
5. J.D. Axe, "The Electronic Structure of Octahedrally Coordinated Protactinium(IV)," 1960, UCRL-9293.
6. J.D. Axe, H.J. Stapleton, and C.D. Jeffries, Phys. Rev. 121, 1630 (1961).
7. N. Edelstein, D. Brown, and B. Whittaker, Inorg. Chem. 13, 1805 (1974).
8. D. Brown, B. Whittaker, and N. Edelstein, Inorg. Chem. 15, 511 (1976).
9. J.C. Krupa, S. Hubert, M. Foyentin, E. Gamp, and N. Edelstein, J. Chem. Phys. 78, 2175 (1983).
10. R.C. Naik and J.C. Krupa, J. Lumin. 31/32, 222 (1984).
11. N. Edelstein, J.C. Krupa, R.C. Naik, K. Rajnak, B. Whittaker, and D. Brown, Inorg. Chem. 27, 3186 (1988).
12. B.G. Wybourne, "Spectroscopic Properties of Rare Earths," Wiley, New York, 1965.
13. B.R. Judd, "Operator Techniques in Atomic Spectroscopy," McGraw Hill, New York, 1963.
14. R.G. Denning, in "Vibronic Processes in Inorganic Chemistry," C.D. Flint, Ed. NATO ASI Series C: Vol. 288, Kluwer, Dordrecht, 1989, p. 111.

15. B. Henderson and G.F. Imbusch, "Optical Spectroscopy of Inorganic Solids," Oxford University Press, Oxford, 1989.

16. G.M. Williams, P.C. Becker, J.G. Conway, N. Edelstein, L.A. Boatner, and M.M. Abraham, Phys. Rev. B 40, 4132 (1989).

17. G.P. O'Leary and R.G. Wheeler, Phys. Rev. B 1, 4409 (1970).

18. D. Brown, B. Whittaker, and P.E. Lidster, "Infrared and Raman Studies on Actinide(IV) Hexahalogeno-Complexes," AERE-R8035, 1975.

19. S.B. Piepho, J.R. Dickinson, J.A. Spencer, and P.N. Schatz, J. Chem. Phys. 57, 982 (1972).

20. K.D. Warren, Inorg. Chem. 19, 653 (1980).

$$\Gamma_7 \quad \begin{vmatrix} 0 & \sqrt{3}\zeta \\ \sqrt{3}\zeta & \Delta-\frac{1}{2}\zeta \end{vmatrix}$$

$$\Gamma_8 \quad \begin{vmatrix} \Delta+\frac{1}{4}\zeta & \frac{3}{4}(\sqrt{5})\zeta \\ \frac{3}{4}(\sqrt{5})\zeta & \Delta+\theta-\frac{3}{4}\zeta \end{vmatrix}$$

$$\Gamma_6 \quad \left|\Delta+\theta+\frac{3}{2}\zeta\right|$$

$$g_{\Gamma_7} = 2(\cos\alpha)^2 - \frac{8}{\sqrt{3}}\sin\alpha\cos\alpha$$

$$\tan 2\alpha = \frac{2(\sqrt{3})\zeta}{\Delta - \frac{1}{2}\zeta}$$

$$b_4 = \frac{1}{33}B_0^4,\ b_6 = (\frac{-5}{429})B_0^6$$

$$\theta = 8b_4 - 56b_6$$

$$\Delta = 10b_4 + 84b_6$$

Table 1. Energy matrices and equations

phonons involved	$6d(\Gamma_{8g})$-$^2F_{5/2}(\Gamma_{7u})$ line position[a] (cm^{-1})	$6d(\Gamma_{8g})$-$^2F_{5/2}(\Gamma_{8u})$ line position (cm^{-1})	$6d(\Gamma_{8g})$-$^2F_{7/2}(\Gamma'_{8u})$ line position (cm^{-1})	$6d(\Gamma_{8g})$-$^2F_{7/2}(\Gamma_{6u})$ line position (cm^{-1})
zero phonon line	19954	17847	12685	11783
ν_{L1}		37	31	
ν_{L2}	48	48	49	49
ν_{100}			106	
ν_5	126	123		132
ν_{170}	174	180		180
ν_2	253	256	252	266
ν_1	310	310	310	310
$\nu_1 + \nu_{L1}$	310 + 34	310+36	310+39	310+36
$\nu_1 + \nu_{L2}$	310 + 48	310+49	310+51	310+47
$\nu_1 + \nu_{100}$			310+102	
$\nu_1 + \nu_5$	310 + 126	310+123		310+130
$\nu_1 + \nu_{170}$	310 + 175	310+170		
$\nu_1 + \nu_2$	310 + 253	310+251	310+253	310+250
$2\nu_1$	2(310)	2(310)	2(310)	2(310)
$2\nu_1 + \nu_{L1}$	2(310) + 36	2(310) + 36	2(310) + 33	
$2\nu_1 + \nu_{L2}$	2(310) + 46	2(310) + 45	2(310) + 49	
$2\nu_1 + \nu_{100}$	2(310) + 105	2(310) + 91	2(310) + 106	
$2\nu_1 + \nu_5$	2(310) + 125	2(310) + 126		
$2\nu_1 + \nu_{170}$	2(310) + 174			
$2\nu_1 + \nu_2$	2(310) + 253			
$3\nu_1$	3(310)	3(310)	3(310)	
$3\nu_1 + \nu_{L1}$		3(310) + 41		
$3\nu_1 + \nu_{L2}$	3(310) + 47			
$3\nu_1 + \nu_{100}$		3(310) + 113		
$3\nu_1 + \nu_5$	3(310) + 125			
$3\nu_1 + \nu_{170}$	3(310) + 168			
$3\nu_1 + \nu_2$	3(310) + 254			
$4\nu_1$	4(310)	4(310)		
$4\nu_1 + \nu_{L1}$	4(310) + 32			
$4\nu_1 + \nu_{100}$		4(310) + 114		
$5\nu_1$		5(310)		

[a]Except for the zero phonon line, the columns represent the difference between the zero phonon line and the vibronic peaks.

Table 2. Measured fluorescent peaks and assignments.

Crystal Field Levels and g value	Energy (cm^{-1}) Axe (1960)	Energy (cm^{-1}) This work	Calculated[c] (cm^{-1})
$6d(\Gamma'_{8g})$		> 33000[b]	
$6d(\Gamma_{7g})$		23000±500[b]	
$6d(\Gamma_{8g})$		19956±3	
$^2F_{7/2}(\Gamma_{6u})$	8121	8173±3	8173
$^2F_{7/2}(\Gamma'_{8u})$	7085	7272±3	7272
$^2F_{7/2}(\Gamma'_{7u})$	5215	5250±50	5539
$^2F_{5/2}(\Gamma_{8u})$	(1912)[a]	2108±1	2108
$^2F_{5/2}(\Gamma_{7u})$	0	0	0
g_{Γ_7}	-1.141±0.002	-	-0.953

[a]calculated by Axe (Ref. 5).

[b]from Ref. 11

[c]Parameters ζ = 1539.6 cm^{-1}, B_0^4 = 6945.3 cm^{-1}, B_0^6 = -162.7 cm^{-1}; or θ = 1577.5 cm^{-1}, Δ = 2263.9 cm^{-1}.

Table 3. Experimental and calculated energy levels and ground state g values.

Final State[a]	Calculated Relative Intensity	Experimental Relative Intensity[b]
Γ_{7u}	1	1
Γ_{8u}	2.8	1.5
Γ'_{7u}	5.9×10^{-3}	9×10^{-3}
Γ'_{8u}	.40	.1
Γ_{6u}	.33	c

[a]The initial state for all transitions is the $6d(\Gamma_{8g})$.

[b]Estimated experimental error is ± 20%.

[c]Due to the sharp drop in photomultiplier sensitivity at these wavelengths a reliable intensity measurement could not be obtained.

Table 4. Experimental and Calculated Relative Intensities of the Electronic Transitions.

List of Figures

Energy Levels of Pa^{4+}/Cs_2ZrCl_6

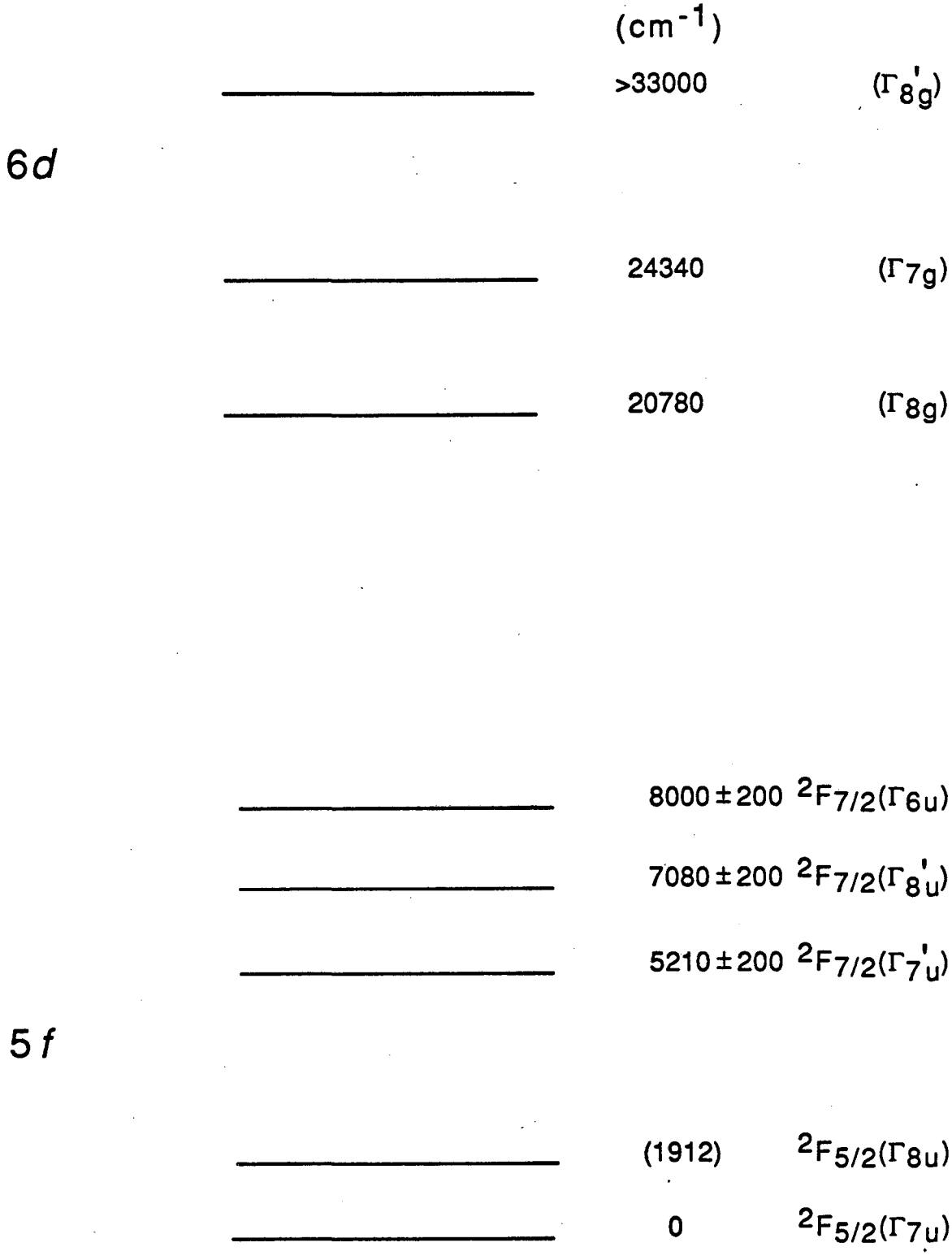

Figure 1

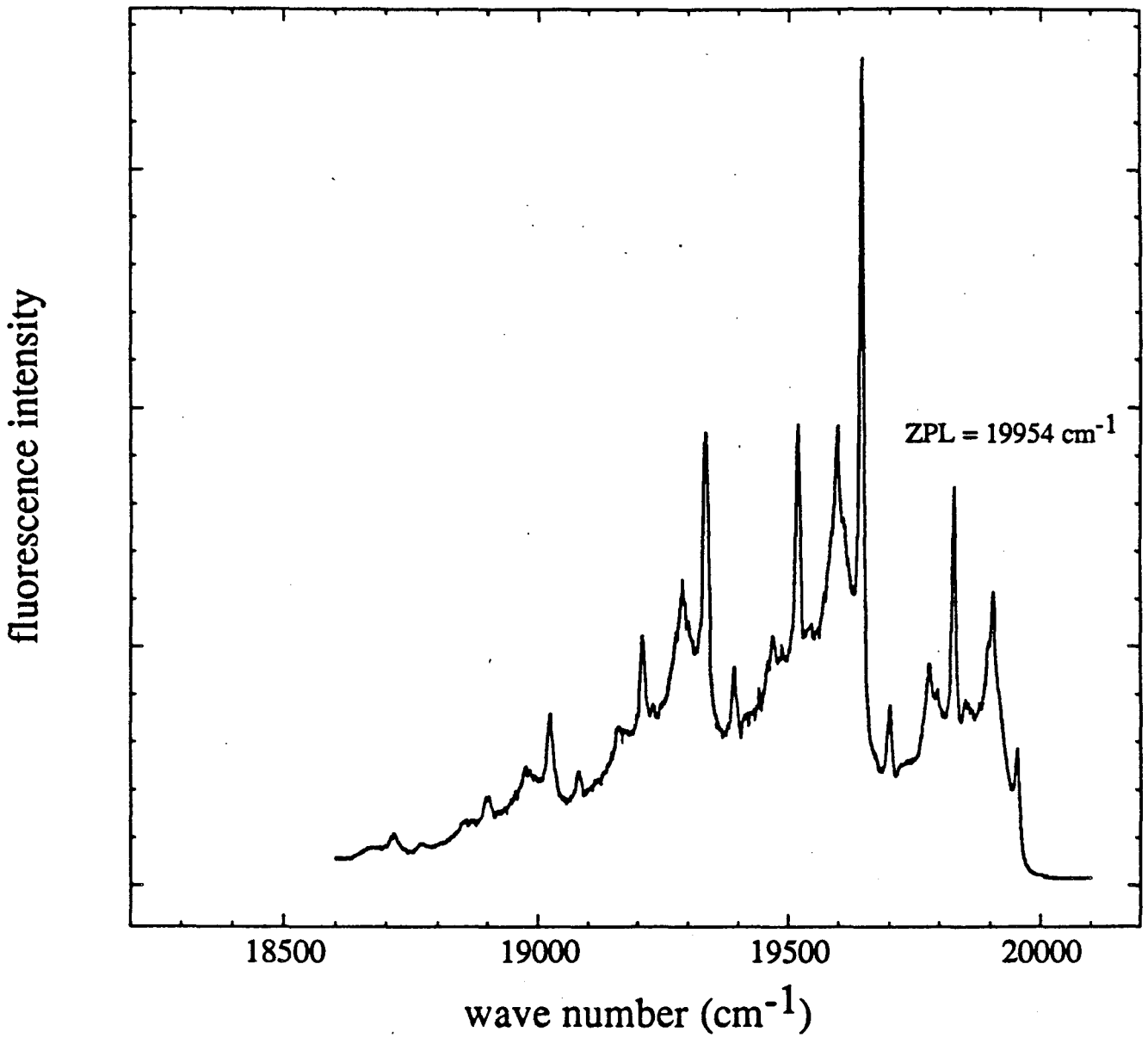
fluorescence intensity
ZPL = 19954 cm-1
18500
19000
19500
20000
wave number (cm-1)

Figure 2

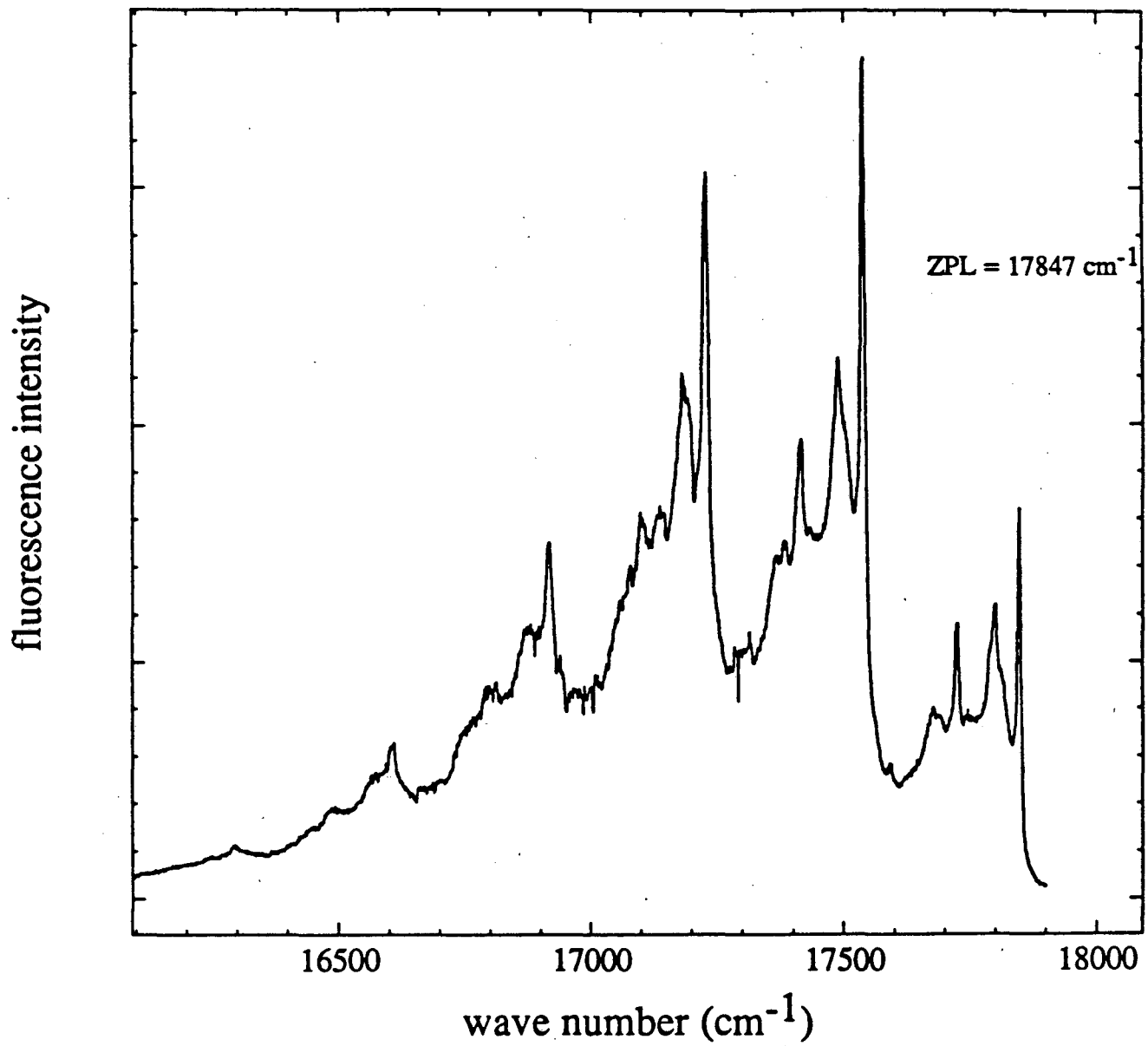
fluorescence intensity
ZPL = 17847 cm-1
16500
17000
17500
18000
wave number (cm-1)

Figure 3

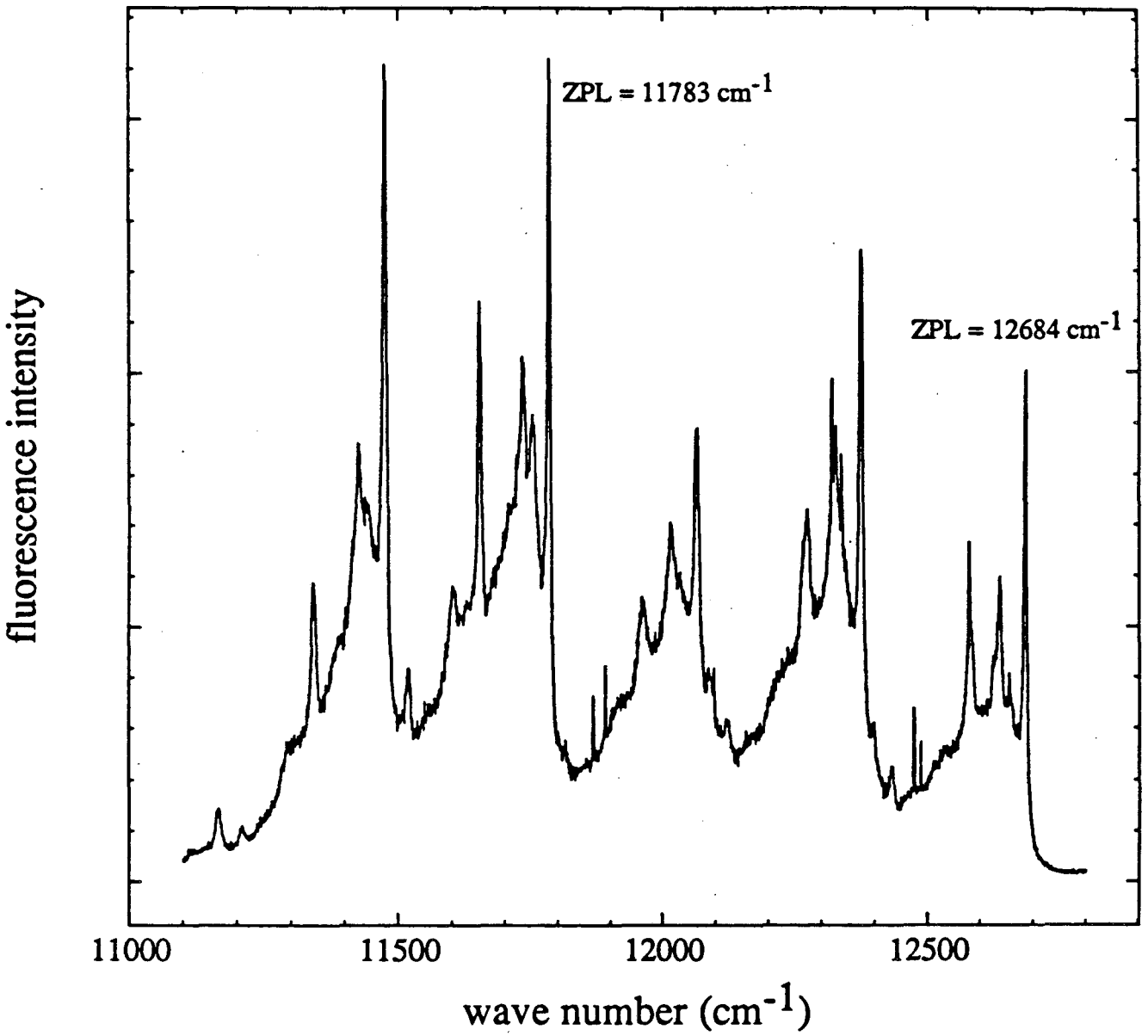
ZPL = 11783 cm-1
ZPL = 12684 cm-1
fluorescence intensity
11000
11500
12000
12500
wave number (cm-1)

Figure 4

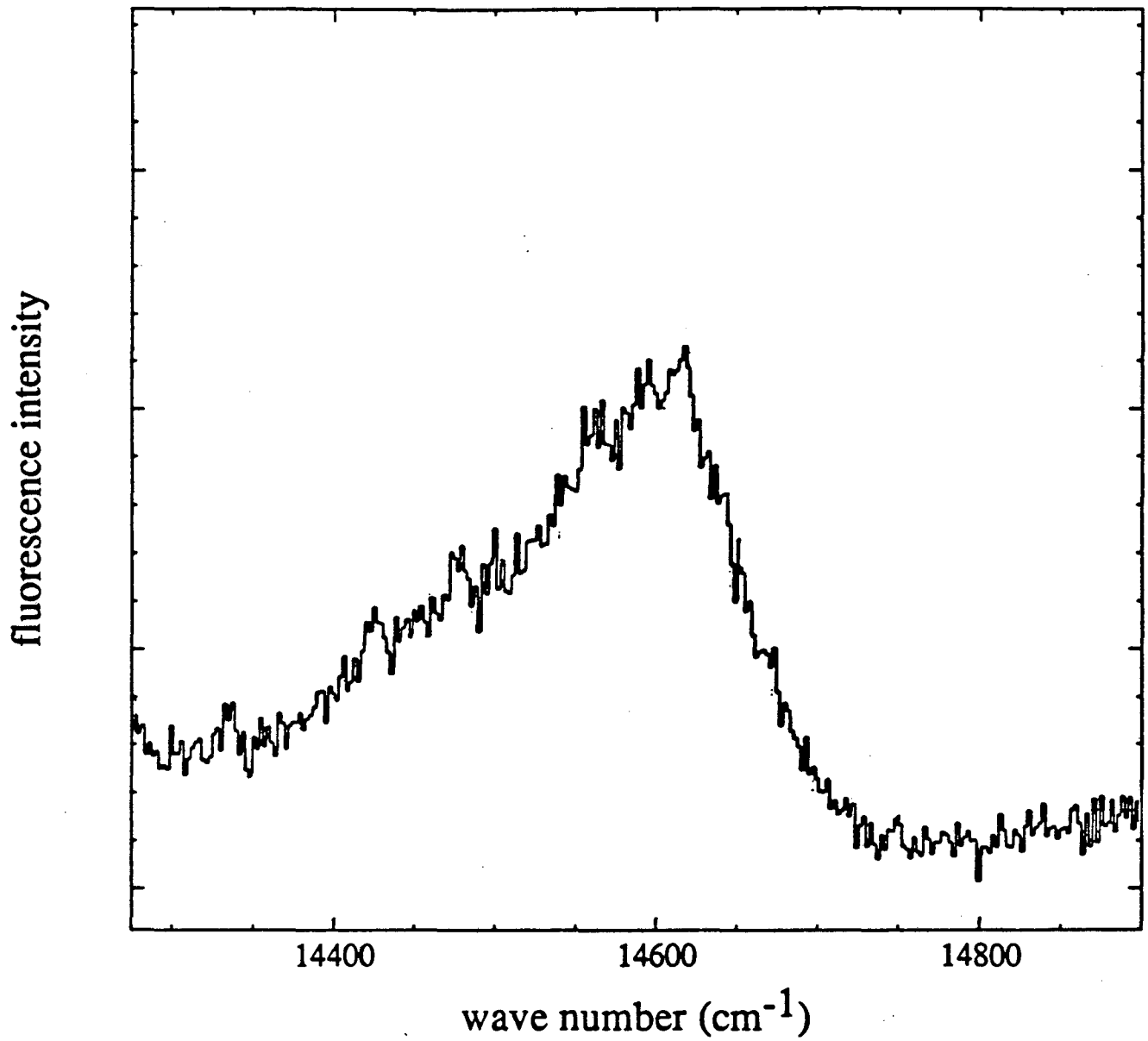

Figure 5

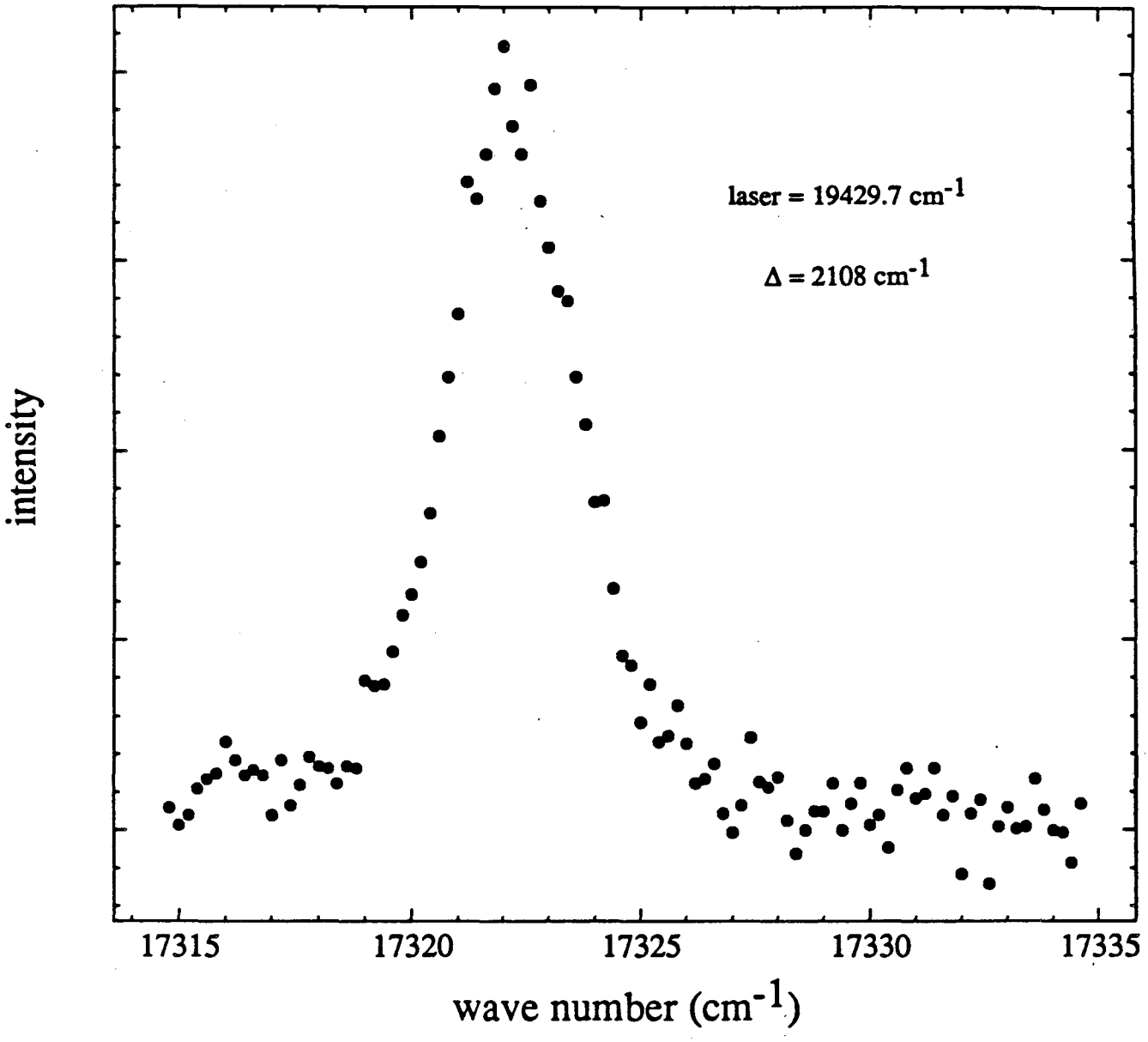
laser = 19429.7 cm-1
Δ = 2108 cm-1
intensity
17315
17320
17325
17330
17335
wave number (cm-1)

Figure 6

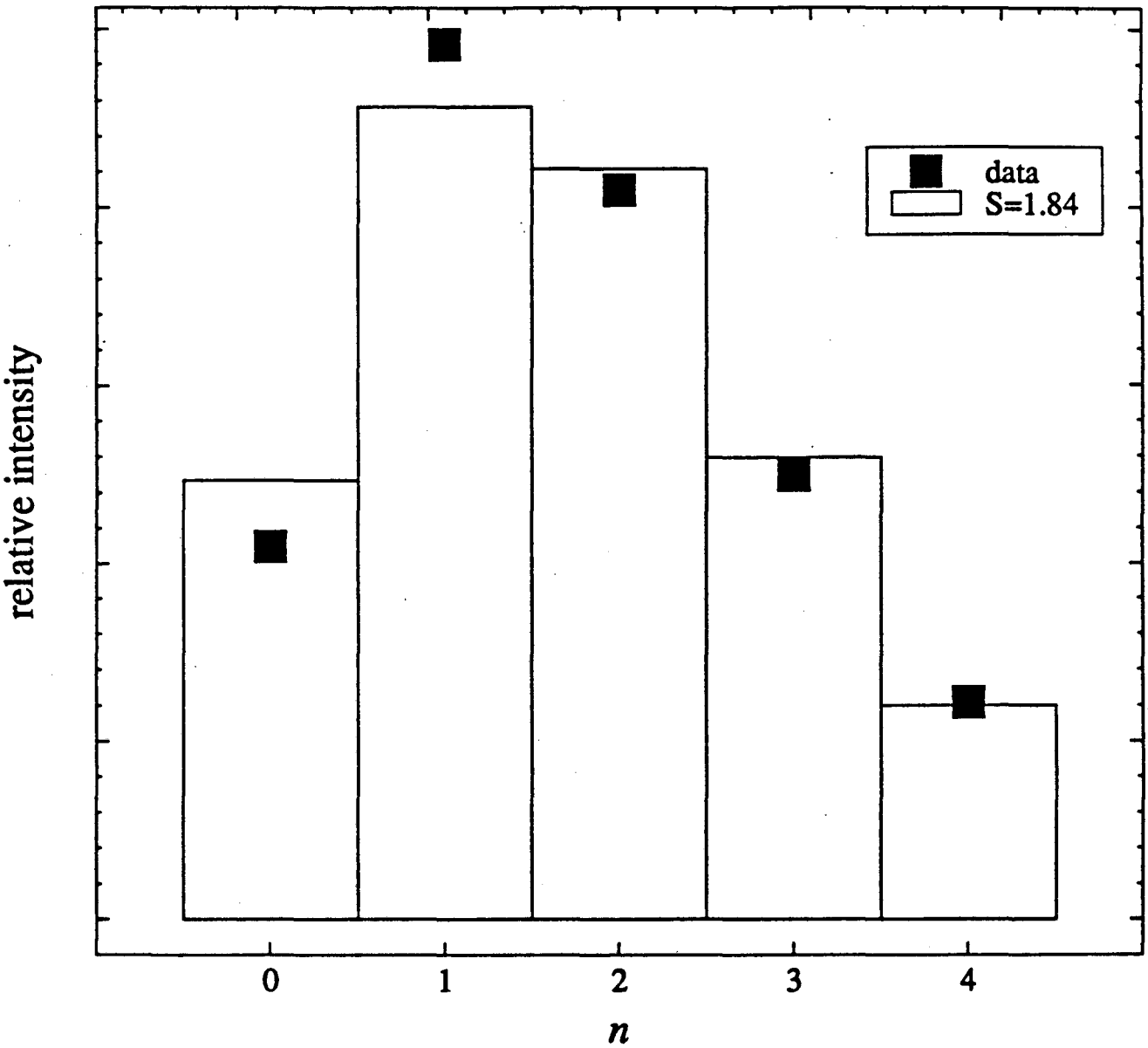

Figure 7

LAWRENCE BERKELEY LABORATORY
UNIVERSITY OF CALIFORNIA
INFORMATION RESOURCES DEPARTMENT
BERKELEY, CALIFORNIA 94720